Development of spiral square coils for magnetic labelling detection in microfluidic systems

Abdelhadi Feddag, Nasr-Eddine Mekkakia-Maaza, Abdelghani Lakhdari

LMSE, Microsystems and Embedded Systems Laboratory, Department of Electronic, Faculty of Electrical Engineering,
University of Science and Technology of Oran, Oran, Algeria

Article Info

ABSTRACT

Due to the development of microfluidic systems biomedical microelectromechanical systems (BioMEMS) for magnetic labelling detection by magnetic microbeads circling in microfluidic channels, we used the magnetic field created by microcoils. The magnetic field associated with the electric current, but with negatively affects if its value increases too much. Handling bio-species in the microfluidic chip requires that the temperature maintained to keep the cells to prevent their destruction. In this paper we have described the spiral square coil design of different structures to produce an effective magnetic flux density. The simulation of the magnetic flux density is carried out with the help of the COMSOL software. We have presented an optimization of the geometric parameters of the microcoil for a better performance and a miniaturization of the structure with copper wire section $S = 25$ µm^2 and inter-wire space $a = 5$ µm. We have also developed this microcoil by adding a ferromagnetic core to the inner center, the results obtained in this work shown that the magnetic flux density increases around 1.07 times in Bx and 1.45 times in Bz. This new approach in designing a microcoil allows to obtaining a fast trapping of the microbeads and a highly sensitive biological element detection and avoiding increase heat ratio in microfluidic systems.

Corresponding Author:

Abdelhadi Feddag
LMSE, Microsystems and Embedded Systems Laboratory, Department of Electronic, Faculty of Electrical
Engineering, University of Science and Technology of Oran
Oran, Algeria
Email: abdelhadi.feddag@univ-usto.dz

1. INTRODUCTION

Microelectromechanical systems (MEMS) are miniaturized devices that integrate electrical and mechanical components at a micronic or submicronics scale. They can include sensors, actuators, and electronic conditioner, withing the same components, and are able performing a wide range of functions such as sensing, actuation, and manipulation of biological cells or tissues in biomedical-microelectromechanical systems (Bio-MEMS) applications. The development of the microfluidic systems components is associated with the microtechnology based on silicon materials. They were developed after the discovery of deep etching and bonding methods [1], [2], which allow to realize microchannels in silicon [3], [4], glass [5], [6], polymer material polydimethylsiloxane (PDMS) [7], [8] and SU-8 [9].

The superparamagnetic particles are tiny magnetic particles (form of microbeads), they exhibit unique magnetic properties, are used by lab-on-chip [10]–[12], for applications in biotechnology, pharmaceuticals, medicine and industry. This type of device was born thirty years ago and is now experiencing tremendous development, through miniaturization of biosensors [13], [14]. Their micronic and nano size and their

manipulation by a magnetic field make them highly required for analysis and diagnosis in biology and medicine [15]–[17].

In the medical field, microbeads can be used to target cells to separate or mark them [18]. Several applications use different ways of transporting the microbeads [19] under the effect of the magnetic field created by a magnet [20] or an electromagnet [21]. The latter allows us to better control the magnetic flux density and to build an integrated microsystem [22], [23] as shown in Figure 1. The aim is to model and simulate a magnetic flux density using the COMSOL Multiphysics software to study the magnetic flux density generated by different square spiral microcoil structures and to study the effects of geometrical and electrical parameters on the behavior of the magnetic flux density.

In general, when using micro-electromagnets for especially magnetic labelling, suffers from many problems, such as coils size and Joule effect heating which are major concerns. Despite these thermal issues, the thermal design of microcoils is scarcely studied. We propose in this paper a new approach in designing microcoil with developed by adding a ferromagnetic core of a nickel-iron material (NiFe) to the inner center for order to increase the magnetic flux density and avoid the effect of the temperature by avoiding increasing the value of the electric current.

This paper is organized into five sections as follows. Section 2 presents the utilization of microbeads for the magnetic labelling detection; it includes the way of manufacturing microbeads for the sake of magnetic labelling functions and so to separate the targeted cells in microfluidic systems. In section 3, we descript the way of designing the microcoil with a demonstration of the different geometrical features, such as the width of the mains input of the injected current, the number of turns, the copper wire section and inter-wire space and the ferromagnetic core. After the designing process by COMSOL Multiphysics software, we made a suitable condition for simulating the magnetic flux density by including the mathematical equations of the microcoil which has been presented in section 4. Finally, section 5 presents the obtained values of the magnetic flux density from the microcoils of different geometrical shapes, along with a discussion of these results.
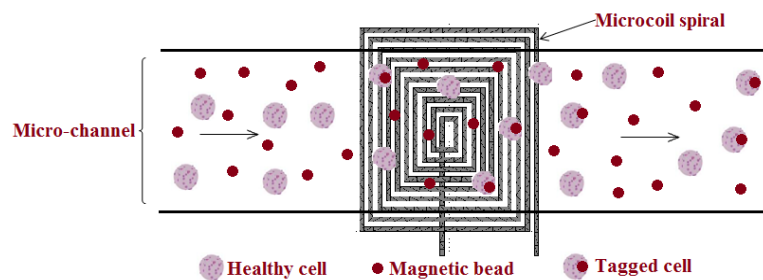

Figure 1. Simple structure of procedural sequences for tagged cell by magnetic bead in the microfluidic system

2. MICROBEADS FOR THE MAGNETIC LABELLING DETECTION

The magnetic labelling detection offers a powerful and versatile tool for sensitive and rapid detection of analysis in various biological and environmental samples. For instance, its usage can extend to every part of the body (blood, saliva, or urine) and are also used by more invasive diagnostic methods (tissue samples) to allow the early diagnosis of disease [24], [25], one of these methods is to use of magnetic beads in the bodily fluids. Protocols involving magnetic microbeads in conventional biological laboratories for capturing proteins, enzymes, ribonucleic acid (RNA) and deoxyribonucleic acid (DNA) are widely used. It is very important to use microbeads in the process of separation in any diagnostic body fluid or target those cells for biomarking (the monocytes in the blood for example), as shown in many works [26], [27], because these magnetic beads are flexible due to the ability of modifying the surface chemistry and the straightforward capturing method by a permanent magnet configuration [28].

This is done in three basic steps. In the first step, in the mixing zone, the antigen of the cells to be targeted is implanted on the surface of the magnetic microbeads and the magnetic microbeads are put into solution to target these cells. Then, in the second step, the target (antigen) contained in the sample is recognized by the probe and adsorbs specifically on the surface of the microbeads (monocyte biomarkers) [29]. Finally, in the separation zone, the magnetic microbeads and labeled monocytes are trapped by a magnetic field generated by permanent magnets [30] or a specially designed microelectromagnet [31]. In the case of permanent magnets, it is possible to structure the magnets in the form of lines and it is also possible to use in the microelectromagnet the microcoils integrated in microfluidic systems [32] with vertical or horizontal separation [33].

3. MODELING OF PLANER SPIRAL SQUARE COILS

Since the magnetic flux density is an essential element in this microfluidic application, and as we are interested in microcoils of squared spiral type, it is important to do predictive calculations concerned with this application. Thus, our purpose is to study the influence of different parameters (number of turns "N", width of the mains input of the injected current "d", copper wire section "S", inter-wire space "a", width of the wire being "r" and the thickness of the wire is "e") on the distribution of the magnetic flux density by using the help of the finite element method (FEM) numerical by COMSOL Multiphysics software in order to evaluate device behavior and to optimize its design. The geometry of the studied model shown in Figure 2 consists of a microcoil of square spiral type with the following geometrical characteristics.
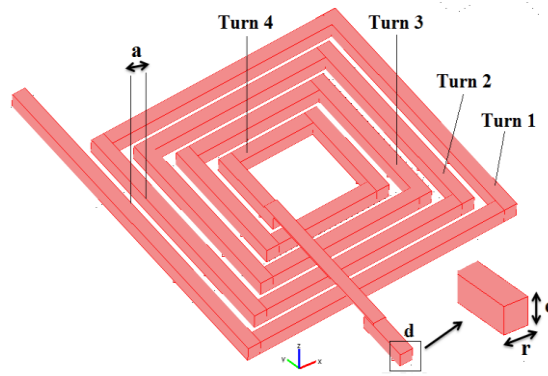

Figure 2. Tridimensional representation of a square spiral microcoil with different parameters

4. METHOD OF CALCULATION

The application of the magnetic flux density B generated by the coils is based on Maxwell's laws, as shown in (1):

$$\nabla . B = 0 \tag{1}$$

This law states that the total magnetic flux through a closed surface is zero. The relationship between the magnetic field H and current density J is given in expression (2):

$$\nabla \times H = J \tag{2}$$

The Biot–Savart law defines the magnetic field H generated at some point in space by a current I, passing in a wire of finite length dl:

$$dH = \frac{I}{4\pi} . \frac{dl \times u}{r^2} \tag{3}$$

where r is the distance from that point to the finite straight wire, u is the displacement vector from the element dl to the point. The relationship between the magnetic field H and the magnetic flux density B is given by (4):

$$B = \mu_0 \mu_r H \tag{4}$$

with $\mu_0 = 4\pi \times 10^{-7}$ H.m^{-1} is the permeability of vacuum and μ_r is the relative permeability.

5. RESULTS AND DISCUSSION

Our first study consists in optimizing of the magnetic flux density for different geometries and then evaluating the magnetic flux density of a selected coil at different heights (h) and electrical parameters (I). The geometries of the models consist of the square spiral type microcoils; their geometric characteristics are shown in Figure 3, which allows us to study the effects of different shapes and dimensions of every coil on the value of the magnetic flux density. To study the impact of the width of the turns on injected current "d", we used the coil in Figure 3(a) with the width of the mains input of the injected current $d = 5$ µm and the coil Figure 3(b) with the width of 40 µm. To study the number of turns "N", we have designed the coil in Figure 3(c) of the

number of turns $N = 3$ and the coil in Figure 3(d) of $N = 5$ turns. The copper wire section "S" is critical in changing the value of the magnetic flux density. Therefore, we designed the coil Figure 3(e) and Figure 3(f) which have the same physical and geometrical characteristics, only the coil in Figure 3(e) is characterized by a different wire section of $S = 5 \times 10$ µm while the coil (f) is $S = 5 \times 5$ µm. Finally, we studied the effect of the inter-wire space "a" where the coil in Figure 3(g) is characterized with the space $a = 5$ µm and the coil Figure 3(h) with space $a = 10$ µm.

$N = 4, r = 5$ µm, $e = 5\,m, a = 5$ µm		$d = 40\,m, r = 5$ µm, $e = 5$ µm, $a = 5$ µm	
$d = 5$	$d = 40$ µm	$N = 3$ turns	$N = 5$
(a)	(b)	(c)	(d)

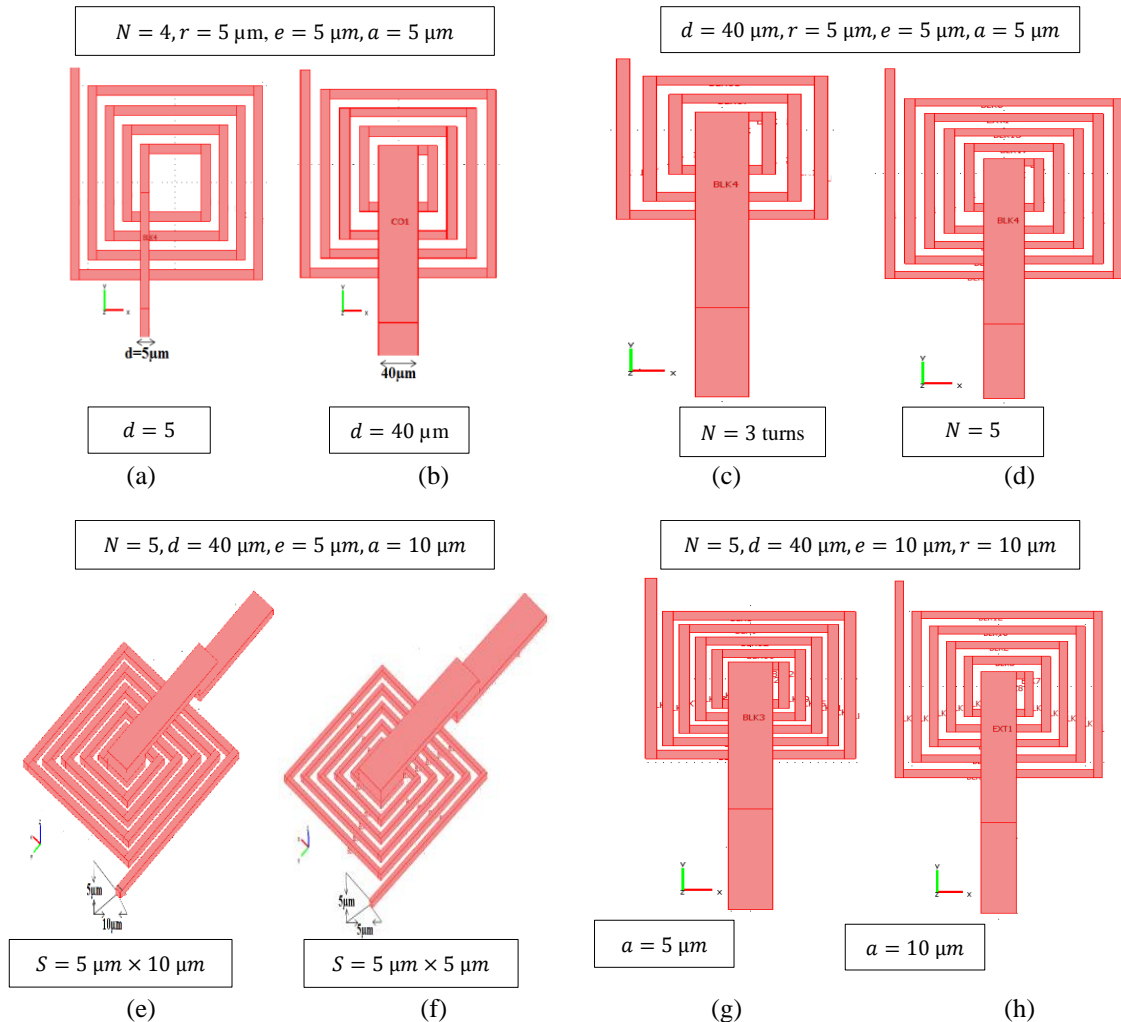| $N = 5, d = 40$ µm, $e = 5$ µm, $a = 10$ µm		$N = 5, d = 40$ µm, $e = 10$ µm, $r = 10$ µm	
$S = 5$ µm $\times$ 10 µm	$S = 5$ µm $\times$ 5 µm	$a = 5\,m$	$a = 10\,m$
(e)	(f)	(g)	(h)

Figure 3. Representation of different parameters of studied microcoils, (a) is characterized by a width of turns 5 µm unlike (b) which is 40 µm, and (c) has 3 turns, while (d) is 5 turns, (e) has section wire of (5×10) µm² and (f) is (5×5) µm², (g) the inter-wire space of 5 µm is different from (h) which is 10 µm

5.1. Effect of design on the magnetic flux density

In this paper, we will discuss the effect of the width of the main input of the injected current and the effect of the number of turns by comparing the magnetic flux density resulting from the coils. Moreover, we will study the effect of the copper wire section and the inter-wire space effect through the values obtained from simulating the magnetic flux density. Finally, we will also examine the effect of the ferromagnetic core on the magnetic flux density value.

5.1.1. Effect of the width of the turns on injected current "d"

The geometrical shape of the microcoil has a crucial effect of the magnetic flux density. For this, we will study the influence of the width of the injected current, we modeled and simulated the magnetic flux density B by two microcoils shown in Figures 3(a) and 3(b), with the same geometrical characteristics ($N = 4, e = 5$ µm, $r = 5$ µm, $a = 5$ µm), but different in the width of the injected current "d", with $d = 5$ µm

in Figure 3(a), and $d = 40$ µm in Figure 3(b). Figure 4 shows the evolution of the magnetic flux density components B_x and B_z behaviors for the two structures along of the microcoil with a 5 and 40 µm width of the injected current fixed at 100 mA at different heights from 5 to 50 µm above the microcoil.
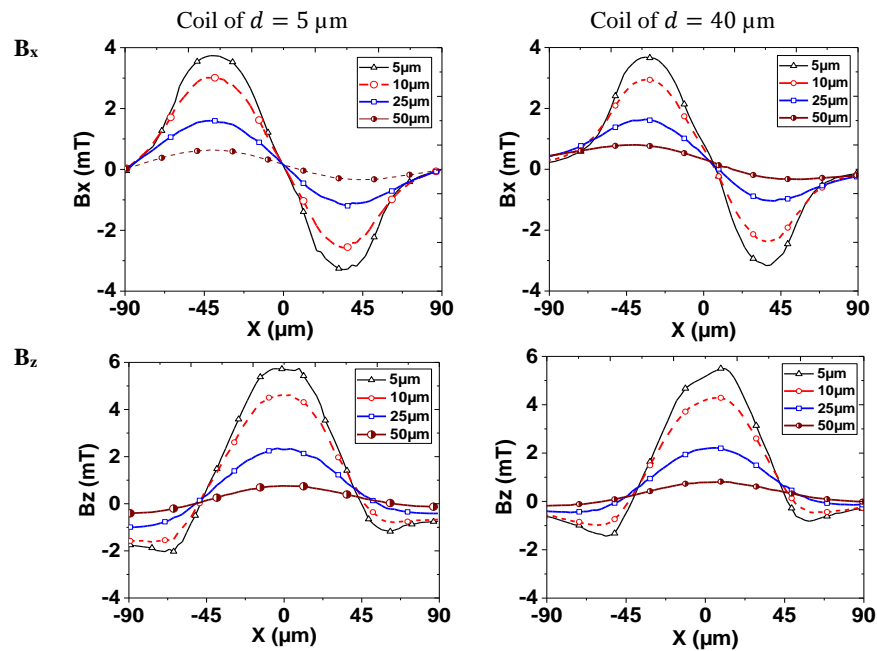

Figure 4. Variation of the magnetic flux density for the two microcoils along of the microcoil with a 5 µm and 40 µm width of the injected current, the current is fixed at 100 mA

After modeling and simulating the magnetic flux density B by two microcoils with different injected current widths, we obtained the maximum magnetic flux density results presented in Table 1. We specifically chose heights of 5 and 50 μm above the microcoil to indicate the respective thicknesses of the channel containing the microfluidics and the microbeads. We note that the variation of the width of the electrical input d results in a weak and negligible increase in the value of the magnetic flux density B_x and B_z.

Table 1. Maximum value of the magnetic flux density component B_x and B_z with different width of injected current (d), the current is fixed at 100 mA

Components of magnetic flux density	Height (µm)	Coil of $N = 4, S = (5 \times 5)$ µm², $a = 5$ µm, $d = 5$ µm (mT)	Coil of $N = 4, S = (5 \times 5)$ µm², $a = 5$ µm, $d = 40$ µm (mT)
B_{xmax}	5	3.73	3.68
	50	0.63	0.80
B_{zmax}	5	5.74	5.49
	50	0.75	0.81

5.1.2. Effect of the number of turns "N"

We then study the effect of another factor in the coil's geometric shape on the magnetic flux density values, namely the number of turns. To do this, two microcoils are optimized with the same geometrical and electrical characteristics, but with a different number of turns for each coil, with $N = 3$ and $N = 5$. In this case, Figure 5 shows the obtained values of the magnetic flux density components B_x and B_z, the current is fixed at 100 mA at different heights from 5 to 50 µm above the microcoil. The maximum values of the magnetic flux density components B_x and B_z are reported in Table 2.

The number of turns in the microcoil significantly effects of the magnetic flux density. We notice that increase in the number of turns, improves the values of the magnetic flux density components B_x and B_z. Thus, when the number of turns increases from 3 to 5, we observe an increase of 1.2 times for the "X" component (3.31 to 3.97 mT), and 1.4 times for the "Z" component (4.49 to 6.36 mT).
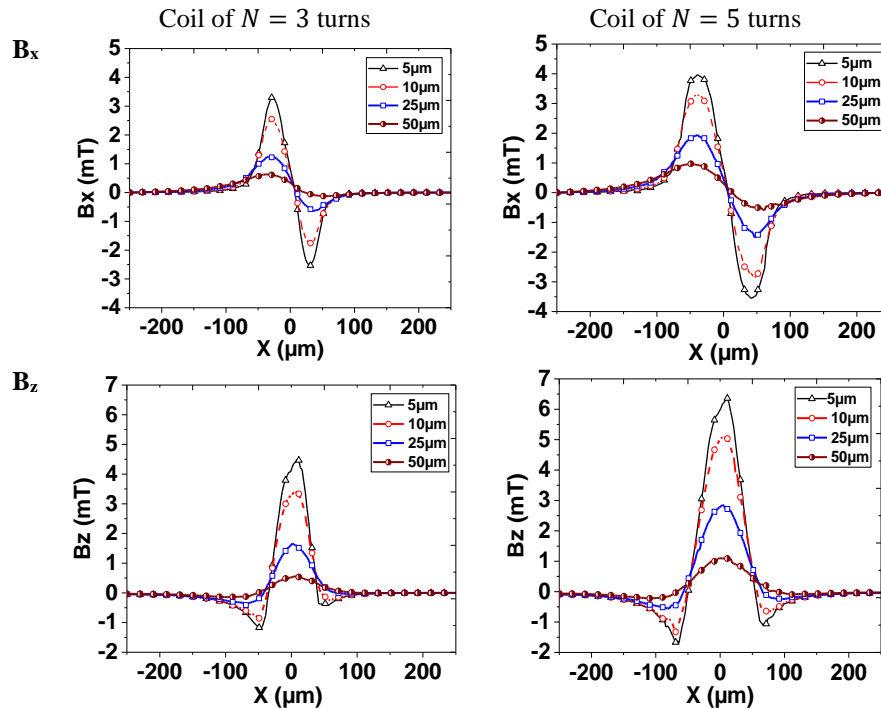
Figure 5. Variation of the magnetic flux density for two microcoils in the 3 and 5 turns with the different heights above the coil, the current is fixed at 100 mA

Table 2. Maximum value of the magnetic flux density component B_x and B_z for two microcoils in the 3 and 5 turns

Components of magnetic flux density	Height (µm)	Coil of $N = 3, S = (5x5)$ µm^2, $a = 5$ µm (mT)	Coil of $N = 5, S = (5x5)$ µm^2, $a = 5$ µm (mT)
B_{xmax}	5	3.31	3.97
	50	0.63	0.98
B_{zmax}	5	4.49	6.36
	50	0.55	1.09

5.1.3. Effect of the copper wire section "S"

Varying the dimensions of the coil cross section has a strong effect on the magnetic flux density of the microcoils. Figure 6 represents the results obtained for the two values of section of the coil (10×5) µm^2 and (5×5) µm^2. The current is fixed at 100 mA at different heights from 5 to 50 µm above the microcoil.

The values of the magnetic flux density components B_x and B_z increase with the decrease of the conductor width from 10 to 5 µm. This is due to the current density which is twice as high between these two structures. A current density of 2×10^9 A/m^2 is injected in the 10 µm wide segment versus 4×10^9 A/m^2 in the 5 µm wide segment. The values are reported in Table 3.

5.1.4. Effect of the inter-wire space "a"

To investigate the effect of the inter-wire space on the magnetic flux density, we have taken into account two special square microcoils of 5 turns made of copper wire section (10×10 µm) and inter-wire space of 5 and 10 µm as shown in Figures 3(g) and 3(h). The variations of the B_x, B_z components at different heights above the microcoil will be shown in Figure 7. The maximum values of magnetic flux density components B_x, B_z are presented in Table 4.

This simulation has allowed us to recognize the importance of the inter-wire spaces to determining the value of the magnetic flux density. We notice the values of the magnetic flux density components B_x, B_z increase weakly for the inter-wire space of the microcoil from 10 to 5µm. Indeed, when the inter-wire space decreases from 10 to 5 µm, the impact of the magnetic flux density component B_x increases by about 1.25 times, and that of the magnetic flux density component B_z by about 1.10 times.
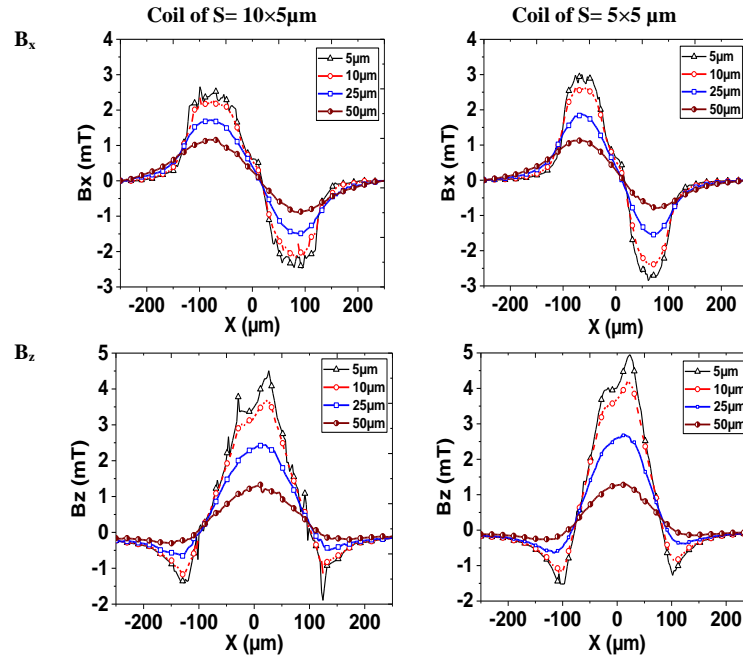
Figure 6. Variation of the magnetic flux density component for two microcoils for $S = 10 \times 5$ µm and $S = 5 \times 5$ µm, the current is fixed at 100 mA

Table 3. The maximum value of magnetic flux density component B_x and B_z at different coil size of copper wire section

Components of magnetic flux density	Height (µm)	Coil of $N = 5, S = (10 \times 5)$ µm², $a = 10$ µm (mT)	Coil of $N = 5, S = (5 \times 5)$ µm², $a = 10$ µm (mT)
B_{xmax}	5	2.65	2.99
	50	1.16	1.12
B_{zmax}	5	4.50	4.94
	50	1.32	1.30

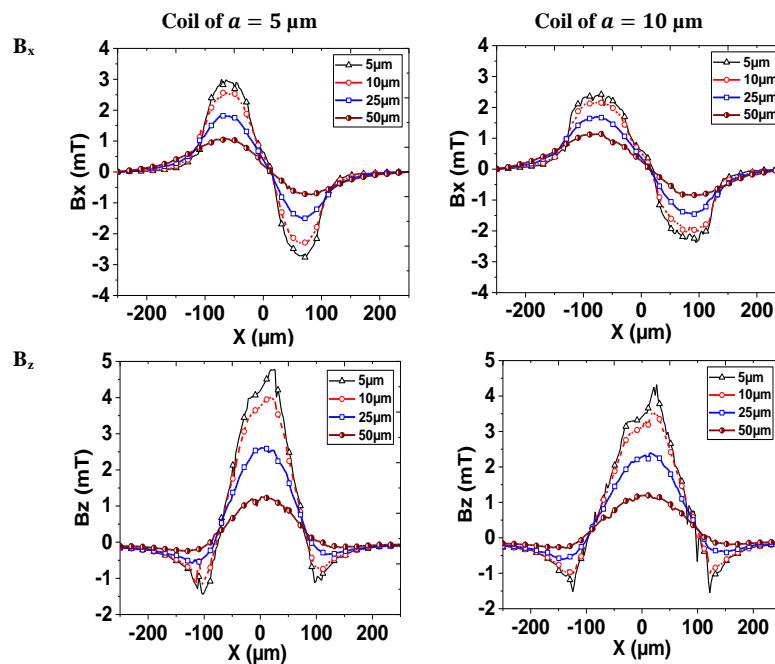Figure 7. Variation of the magnetic flux density component for two microcoils consisting of the inter-wire spaces $a = 5$ µm and $a = 10$ µm, the current is fixed at 100 mA

Table 4. The maximum values of magnetic flux density components B_x, B_z with different in the inter-wire space, the injected current $I = 100$ mA

Components of magnetic flux density	Height (µm)	Coil of $N = 5, S = (10 \times 10)$ µm², $a = 5$ µm (mT)	Coil of $N = 5, S = (10 \times 10)$ µm², $a = 10$ µm (mT)
B_{xmax}	5	2.99	2.41
	50	1.09	1.13
B_{zmax}	5	4.77	4.32
	50	1.25	1.19

5.1.5. Effect of the ferromagnetic core

The geometrical shape of the microcoil is an important factor in enhancing the magnetic flux density. However, the values of the magnetic flux density may not be sufficient for labelling and separating the cells in microfluidic systems. To address this, we can enhance the coils by incorporating a ferromagnetic core. The comparison between the magnetic flux density variations of the two microcoils is shown in Figure 8. A simulation using COMSOL software was conducted to study the influence of the ferromagnetic core located in the middle of the microcoil center represented in Figure 8(a). The ferromagnetic core is a cube-shaped nickel-iron (NiFe) material with a thickness of 20 µm. This microcoil has the same geometrical and electrical properties as the microcoil without core in Figure 8(b). The current is fixed at 100 mA at different heights from 5 to 50 µm above the microcoil. The maximum values of magnetic flux density components B_x, B_z are presented in Table 5.
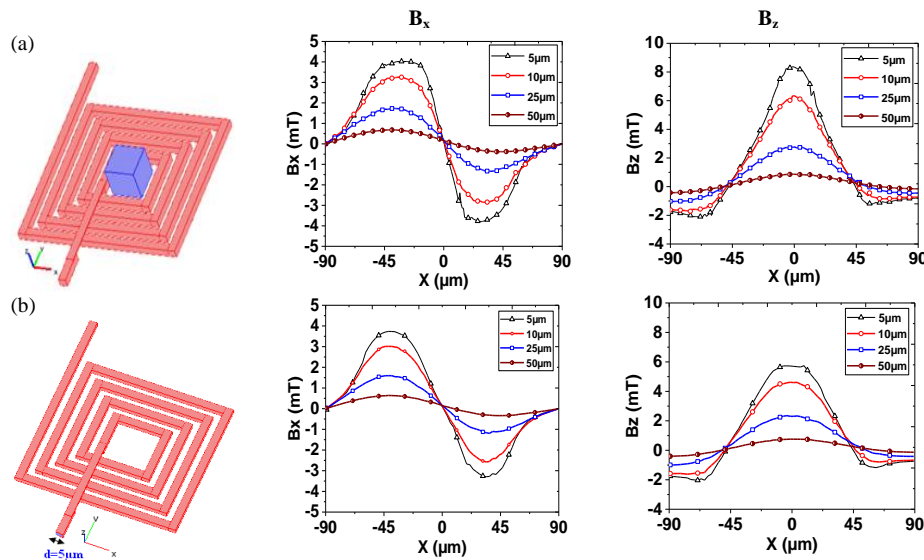

Figure 8. Variation of the magnetic flux density component B_x, B_z, for two microcoil, (a) variation of the magnetic flux density by micro coil with ferromagnetic core and (b) variation of the magnetic flux density by microcoil without core, the current is fixed at 100 mA

Table 5. The maximum value of magnetic flux density component B_x and B_z for two microcoils with ferromagnetic core in the first coil, the current is fixed at 100 mA

Components of magnetic flux density	Height (µm)	Microcoil and ferromagnetic (mT)	Microcoil (mT)
B_{xmax}	5	4.02	3.73
	50	0.68	0.63
B_{zmax}	5	8.37	5.74
	50	0.87	0.75

The magnetic flux density values obtained in Table 5 confirm that the incorporation of a ferromagnetic core in the center of the microcoil plays a crucial role to obtain an efficient magnetic flux density. We notice that the addition of the ferromagnetic core allowed the increase of the value of the magnetic flux density for B_x, and for B_z. In fact, the impact of the magnetic flux density B_x increases around 1.07 times, and the component of the B_z increases around 1.45 times. On the other hand, we notice that in Figure 8, the shape of the magnetic flux density is not modified.

6. CONCLUSION

In this paper, we have investigated the effects of different geometrical properties of spiral square microcoils type on the induced magnetic flux density. This study allows us to give a preview of the geometric characteristics of the coil that must be manufactured to have an effective magnetic flux density on the level of the microchannel systems for magnetic labeling's sake and for separating targeted cells. We have also studied the effects of current input and ferromagnetic materials. The calculations have been carried out with the help of COMSOL Multiphysics software.

We have noted that changing the width of the mains input of the injected current gives just a small, non-considerable variation in the value of the magnetic flux density. We noted that an increase in the number of turns, leads to a significant increase in the components of the magnetic flux density B_x and B_z. When we vary the copper wire section, the values of the magnetic flux density remain approximately constant for different sizes when the height is higher (50 µm), but for a low height (5 µm), the magnetic flux density maxima are greater for lower size. The influence of the inter-wires space seems also to be insignificant for great height (50 µm), but not for low heights (5 µm) for which, the components of the magnetic flux density increase with decreasing the inter-spacing turns between each conductor line. We have proposed a new technique for designing and optimizing of the microcoil with introduction of a ferromagnetic core of a nickel-iron (NiFe) material that leads to a significant increase of the magnetic flux density. This new approach in designing of microcoil is considered the best to obtain a fast trapping of the microbeads and highly sensitive detection of biological elements and to avoid the effect of temperature in microfluidic systems.

REFERENCES

[1] T. Ju, "Working principle and applications of active and passive microfluidic valves," *Journal of Physics: Conference Series*, vol. 2230, no. 1, Mar. 2022, doi: 10.1088/1742-6596/2230/1/012013.

[2] C. Huo, C. Bai, and P. Zhang, "Micropumps for microfluidic devices and BioMEMS," *Journal of Physics: Conference Series*, vol. 1626, no. 1, Oct. 2020, doi: 10.1088/1742-6596/1626/1/012040.

[3] M. A. Moyet *et al.*, "MEMS micromixer for ultra fast mixing of fluids," in *2020 IEEE 33rd International Conference on Micro Electro Mechanical Systems (MEMS)*, Jan. 2020, pp. 1137–1140, doi: 10.1109/MEMS46641.2020.9056400.

[4] A. Gupta, P. Sundriyal, A. Basu, K. Manoharan, R. Kant, and S. Bhattacharya, "Nano-finishing of MEMS-based platforms for optimum optical sensing," *Journal of Micromanufacturing*, vol. 3, no. 1, pp. 39–53, May 2020, doi: 10.1177/2516598419862676.

[5] M. Zhang *et al.*, "Research on the protrusions near silicon-glass interface during cavity fabrication," *Micromachines*, vol. 10, no. 6, Jun. 2019, doi: 10.3390/mi10060420.

[6] T. Tang, Y. Yuan, Y. Yalikun, Y. Hosokawa, M. Li, and Y. Tanaka, "Glass based micro total analysis systems: Materials, fabrication methods, and applications," *Sensors and Actuators B: Chemical*, vol. 339, Jul. 2021, doi: 10.1016/j.snb.2021.129859.

[7] K. Raj M and S. Chakraborty, "PDMS microfluidics: A mini review," *Journal of Applied Polymer Science*, vol. 137, no. 27, Jul. 2020, doi: 10.1002/app.48958.

[8] D. Ficai *et al.*, "Microelectromechanical systems based on magnetic polymer films," *Micromachines*, vol. 13, no. 3, Feb. 2022, doi: 10.3390/mi13030351.

[9] Q. Chen, J. Zhou, Q. Zheng, and Y. Hu, "Multi-layer lithography using focal plane changing for SU-8 microstructures," *Materials Research Express*, vol. 7, no. 6, Jun. 2020, doi: 10.1088/2053-1591/ab98cc.

[10] Y. Ha *et al.*, "Recent advances incorporating superparamagnetic nanoparticles into immunoassays," *ACS Applied Nano Materials*, vol. 1, no. 2, pp. 512–521, Feb. 2018, doi: 10.1021/acsanm.7b00025.

[11] Z. Liu, A. Fornell, and M. Tenje, "A droplet acoustofluidic platform for time-controlled microbead-based reactions," *Biomicrofluidics*, vol. 15, no. 3, May 2021, doi: 10.1063/5.0050440.

[12] B. Düsenberg, P. Groppe, S. Müssig, J. Schmidt, and A. Bück, "Magnetizing oolymer oarticles with a solvent-free single stage orocess using superparamagnetic iron oxide nanoparticles (SPIONs)," *Polymers*, vol. 14, no. 19, Oct. 2022, doi: 10.3390/polym14194178.

[13] I. Dutta *et al.*, "Review on application of Bio-MEMS," *International Journal of Innovative Research in Electrical, Electronics, Instrumentation and Control Engineering*, vol. 9, no. 1, pp. 55–59, 2021.

[14] C. Chircov and A. M. Grumezescu, "Microelectromechanical systems (MEMS) for biomedical applications," *Micromachines*, vol. 13, no. 2, Jan. 2022, doi: 10.3390/mi13020164.

[15] B. N. Zhao, "Efficient particle separation in microfluid channel with inhomogeneous magnetic field," *Journal of Electromagnetic Analysis and Applications*, vol. 11, no. 02, pp. 17–23, 2019, doi: 10.4236/jemaa.2019.112002.

[16] S. Yao, Y. Yu, S. Qin, D. Wang, P. Yan, and Z. Zhang, "Research on optimization of magnetic field sensing characteristics of PCF sensor based on SPR," *Optics Express*, vol. 30, no. 10, May 2022, doi: 10.1364/OE.456924.

[17] H. Fan *et al.*, "Detection techniques of biological and chemical Hall sensors," *RSC Advances*, vol. 11, no. 13, pp. 7257–7270, 2021, doi: 10.1039/D0RA10027G.

[18] O. Civelekoglu, A. B. Frazier, and A. F. Sarioglu, "The origins and the current applications of microfluidics-based magnetic cell separation technologies," *Magnetochemistry*, vol. 8, no. 1, Jan. 2022, doi: 10.3390/magnetochemistry8010010.

[19] C. González Fernández *et al.*, "Continuous-flow separation of magnetic particles from biofluids: How Does the microdevice geometry determine the separation performance?," *Sensors*, vol. 20, no. 11, May 2020, doi: 10.3390/s20113030.

[20] L. Descamps *et al.*, "Self-assembled permanent micro-magnets in a polymer-based microfluidic device for magnetic cell sorting," *Cells*, vol. 10, no. 7, Jul. 2021, doi: 10.3390/cells10071734.

[21] A. T. Ajiboye, J. F. Opadiji, J. O. Popoola, and O. Oniyide, "Optimum design of square air-core electromagnetic coil system," *FUOYE Journal of Engineering and Technology*, vol. 6, no. 3, Sep. 2021, doi: 10.46792/fuoyejet.v6i3.662.

[22] G.-P. Zhu, Q.-Y. Wang, Z.-K. Ma, S.-H. Wu, and Y.-P. Guo, "Droplet manipulation under a magnetic field: A review," *Biosensors*, vol. 12, no. 3, Mar. 2022, doi: 10.3390/bios12030156.

[23] R. Abedini-Nassab, M. P. Miandoab, and M. Şaşmaz, "Microfluidic synthesis, control, and sensing of magnetic nanoparticles: A review," *Micromachines*, vol. 12, no. 7, Jun. 2021, doi: 10.3390/mi12070768.

[24] X. Xue, H. Ye, and Z. Hu, "Microfluidic system for cell sorting," *Journal of Physics: Conference Series*, vol. 2012, no. 1, Sep. 2021, doi: 10.1088/1742-6596/2012/1/012129.

[25] S. M. Ali, S. B. Attallah, and S. H. Karim, "Design and fabrication of a nano-microfluidic device for blood and cancer cells separation," *IOP Conference Series: Materials Science and Engineering*, vol. 1094, no. 1, Feb. 2021, doi: 10.1088/1757-899X/1094/1/012053.

[26] L. Descamps, D. Le Roy, C. Tomba, and A. Deman, "Magnetic polymers for magnetophoretic separation in microfluidic devices," *Magnetochemistry*, vol. 7, no. 7, Jul. 2021, doi: 10.3390/magnetochemistry7070100.

[27] D. D. Stueber, J. Villanova, I. Aponte, Z. Xiao, and V. L. Colvin, "Magnetic nanoparticles in biology and medicine: Past, present, and future trends," *Pharmaceutics*, vol. 13, no. 7, Jun. 2021, doi: 10.3390/pharmaceutics13070943.

[28] U. Sajjad *et al.*, "Efficient flowless separation of mixed microbead populations on periodic ferromagnetic surface structures," *Lab on a Chip*, vol. 21, no. 16, pp. 3174–3183, 2021, doi: 10.1039/D1LC00161B.

[29] M.-J. Shen, R. C. L. Olsthoorn, Y. Zeng, T. Bakkum, A. Kros, and A. L. Boyle, "Magnetic-activated cell sorting using coiled-coil peptides: an alternative strategy for isolating cells with high efficiency and specificity," *ACS Applied Materials and Interfaces*, vol. 13, no. 10, pp. 11621–11630, Mar. 2021, doi: 10.1021/acsami.0c22185.

[30] A. Mishra *et al.*, "Ultrahigh-throughput magnetic sorting of large blood volumes for epitope-agnostic isolation of circulating tumor cells," in *Proceedings of the National Academy of Sciences*, vol. 117, no. 29, pp. 16839–16847, Jul. 2020, doi: 10.1073/pnas.2006388117.

[31] R. R. S. Sarreal, D. T. Blake, and P. T. Bhatti, "Development and characterization of a micromagnetic alternative to cochlear implant electrode arrays," *IEEE Transactions on Neural Systems and Rehabilitation Engineering*, vol. 30, pp. 2116–2125, 2022, doi: 10.1109/TNSRE.2022.3193342.

[32] O. Lefebvre *et al.*, "Reusable embedded microcoils for magnetic nano-beads trapping in microfluidics: magnetic simulation and experiments," *Micromachines*, vol. 11, no. 3, Feb. 2020, doi: 10.3390/mi11030257.

[33] M. Frenea-Robin and J. Marchalot, "Basic principles and recent advances in magnetic cell separation," *Magnetochemistry*, vol. 8, no. 1, Jan. 2022, doi: 10.3390/magnetochemistry8010011.

BIOGRAPHIES OF AUTHORS

Abdelhadi Feddag received a Teaching Degree in Technology from (ENSET) Higher Normal School of Technological Education of Oran, Algeria, in 2009. He conducted research in the study of the action of the magnetic fields in microfluidic systems from which he received a magister degree of Physics and Chemics from (ENPO) National School of Polytechnic in Oran, in 2014. He is currently Ph.D. student in the LMSE laboratory, (Microsystems and Embedded Systems Laboratory) in the Electronics Department at the University of Science and Technology Mohamed Boudiaf (USTO-MB) in Oran, Algeria, conducting research in the development of microfluidic microsystems for biomarkers detection. He can be contacted at email: abdelhadi.feddag@univ-usto.dz.

Nasr-Eddine Mekkakia-Maaza received the Post graduate degree on solid state from Oran University, Algeria, in 1986 and Magister in Microelectronics from the Center for Development of Advanced Technologies, Algiers, Algeria in 1990 and Ph.D. degree in microelectronics from University of Science and Technology of Oran (USTO-MB) in 2004. He is currently a professor in Electronics Department at University of Science and Technology of Oran (USTO-MB) and a head of Microsystems and Embedded Systems Laboratory (LMSE). His research interests include micro and nano technologies, mems and microfluidics technology, biosensors, lab on chip, cryogenic plasma etching, plasma etching, reactor engineering, thin films. He can be contacted at email: nasreddine.mekkakia@univ-usto.dz.

Abdelghani Lakhdari receives the Dipl. Eng. Degree in electronic engineering, the Magister degree and the doctorate in micro-electronics from University of Science and Technology Mohamed Boudiaf (USTO-MB), Oran, Algeria in 2010, 2014 and 2020 respectively. He is currently studying and a member in the laboratory of microsystems and embedded systems at the University of Science and Technology Mohamed Boudiaf (USTO-MB) in Oran, Algeria. His research interests are on the subjects of MEMS, microfluidics and wireless power transfer biomedical applications. He can be contacted at email: abdelghani.lakhdari@univ-usto.dz.